K. Heckmann and *Q. Saifi*

Comparative analysis of deterministic and probabilistic fracture mechanical assessment tools

Uncertainties in material properties, manufacturing processes, loading conditions and damage mechanisms complicate the quantification of structural reliability. Probabilistic structure mechanical computing codes serve as tools for assessing leak- and break probabilities of nuclear piping components. Probabilistic fracture mechanical tools were compared in different benchmark activities, usually revealing minor, but systematic discrepancies between results of different codes. In this joint paper, probabilistic fracture mechanical codes are compared. Crack initiation, crack growth and the influence of in-service inspections are analyzed. Example cases for stress corrosion cracking and fatigue in LWR conditions are analyzed. The evolution of annual failure probabilities during simulated operation time is investigated, in order to identify the reasons for differences in the results of different codes. The comparison of the tools is used for further improvements of the codes applied by the partners.

Vergleich probabilistischer und deterministischer Bruchmechanik-Codes. *Unsicherheiten in Werkstoffeigenschaften, Herstellungsprozessen, Lastbedingungen und Schädigungsmechanismen beeinflussen die Quantifizierung der Strukturzuverlässigkeit. Computercodes für probabilistische Strukturmechanik wurden als Werkzeuge zur Bewertung kerntechnischer Rohrleitungskomponenten entwickelt und in verschiedenen Benchmarks verglichen, in denen üblicherweise geringe, aber systematische Unterschiede zwischen verschiedenen Programmen gefunden wurden. In diesem Artikel werden bruchmechanische Analysewerkzeuge verglichen. Die Fallstudien umfassen Rissinitiierung, Risswachstum und wiederkehrende Prüfungen, Testfälle für Spannungsrisskorrosion und Ermüdung in Leichtwasserreaktor-Bedingungen werden analysiert, die Ergebnisse für den Verlauf der jährlichen Versagenswahrscheinlichkeit während des simulierten Betriebs werden verglichen, um die Ursachen für Unterschiede zu identifizieren. Die Vergleichsstudie wird für die Weiterentwicklungen der Programme verwendet.*

1 Introduction

Nuclear components such as pressure vessels and piping of the coolant loop fulfill high safety requirements. This guarantees that the probability of a failure (leak, rupture) is very small. The quantification of this reliability, i.e. the failure probability, is required for several safety standards (where a limiting probability is prescribed), for risk-based inspection approaches (for increasing the efficiency of in-service inspections), for probabilistic safety analyses (where it enters in failure trees), and for sensitivity analyses (identifying the crucial parameters of a component).

Reliability, expected lifetime and failure probability of a structure result from different uncertain influence factors. The material properties of the structure, geometric deviations from the nominal dimensions, degradation mechanisms, defect sizes, operational loading, accident conditions, and inspection efficiency may be characterized by distributed values. The interference of the different scattered parameters gives rise to the probability of safe operation or failure (see Fig. 1).

A key ingredient of the reliability computation for primary circuit components in nuclear power plants is the fracture mechanical description of the evolution of a structure containing a crack. The computation of fracture mechanical parameters, crack growth velocities and the prediction of a possible leakage require nontrivial mathematical formulations. Additionally, the treatment of the uncertain parameters and their distribution functions requires many independent simulations, making use of different methods to increase the computation efficiency. Hence, a number of tools have been developed by technical safety organizations (TSOs) and others in different countries, incorporating the necessary features.

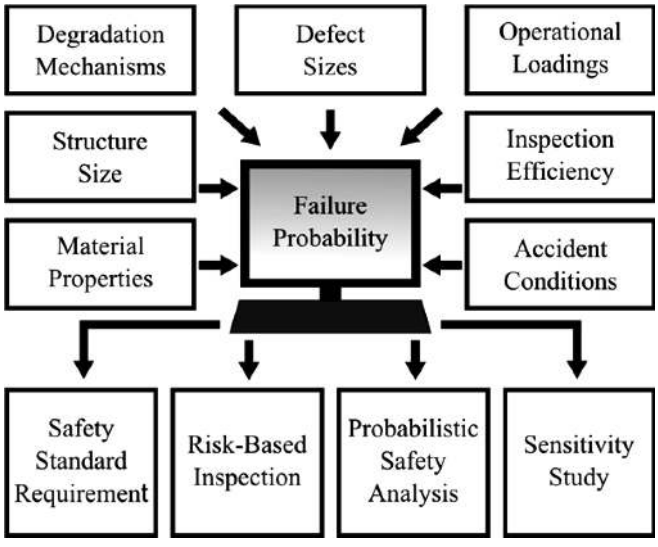

Fig. 1. Failure probability computation. A key role for different applications

The existence of independent code systems which can be addressed to the same type of studies and problem cases motivated a number of benchmark activities in the past [1–3]. These benchmarks compared the results of different codes obtained for selected example cases. The investigated piping components represent different locations in PWR and BWR primary loops, and dealt with crack initiation, fatigue crack growth, environmental assisted fatigue and stress corrosion cracking as damage mechanisms. Although these studies can be seen as successful validations of the participating computing tools, systematic discrepancies between different approaches were observed, especially present in the temporal evolution of the failure probability during the simulated operation period. A systematic investigation of the reasons for differing computation results did not take place.

Nowadays, comparative studies should focus more on the analysis of deviations of the result. One example is the activity Bench-KJ [4], where international partners (and within European TSOs) compare their methodologies for fracture mechanical parameters. The evaluation of the different approaches applied by the partners gave rise to a fruitful discussion of influencing effects and origins of discrepancies [5–7].

The aim of this collaborative paper is the comparison of two fracture mechanical assessment tools developed by the two European TSOs GRS and VTT within a benchmark study. The analysis of the results contains a detailed discussion of the moderate differences in the results and the identification of the key ingredients which are relevant for this finding.

The article is organized as follows. In Sec. 2, the applied codes PROST and VTTBESIT are presented in short. The example cases for comparative calculations are described in Sec. 3, the results of the computations are found in Sec. 4. The comparison and discussion of the results are contained in Sec. 5. The paper concludes with a summary and outlook in Sec. 6.

2 Presentation of the applied codes/approaches

The relevant scope of the two codes under investigation is the structural reliability computation of pressurized components by simulating cracks and their behavior during the load history of the lifetime. Crack initiation during operation as well as flaws resulting from manufacturing processes are investigated, and fatigue crack growth as well as stress corrosion cracking can be assessed.

2.1 PROST (GRS)

The PROST code (**PRO**bablistic **ST**ructural Mechanics) is a tool for the simulation of cracked and uncracked pipes, vessels, and weld joints. More complex components can be analyzed by coupled finite elements approaches. The application can be probabilistic (e.g. for the computation of leak- and break frequencies) or deterministic (e.g. for the simulation of specific configurations).

The PROST software allows the fracture mechanical simulation of flawed structures in multiple topological stages: for example surface flaws which initiate during operation, and further result in a leak, which may cause a rupture. The available degradation mechanisms are fatigue (for fatigue life analysis as well as cyclic crack growth), corrosion (for determination of initiation rates and assessment of stress corrosion cracking) and ductile tearing. The consequences of each damage mechanism can be determined by different models, which are adjustable to a specific situation. Moreover, PROST can be used for leak before break analysis, since leakage rate may be computed and compared to the detection threshold of a leak monitoring system.

The fracture mechanical implementations are based on different compendia and standards, allowing a comparison of different approaches [8–13]. The user is free to use different failure criteria, such as R6/SINTAP/FITNET-based failure assessment diagrams (FAD), geometrical criteria, and critical size implementations.

The leakage flow rate can be computed using inbuilt methods or by coupling with the WinLeck code [14], allowing the comparison of different discharge flow models with respect on regulations given in the new German safety standard KTA 3206 [9]. Probabilistic simulations are performed efficiently with different sampling methods like Monte-Carlo, Stratification Strategies, first order reliability method (FORM), Spherical Sampling, Importance Sampling, Vegas, and others.

A special emphasis is put on the definition of the load sequence, allowing a wide range of operation cycles, detailed load-time functions, special accident conditions, and fatigue load collectives. Data import and rain flow counting is supported for the analysis of complex fatigue loads.

PROST has been validated by reference cases from international benchmark activities, by measurements of experimental investigations, and by comparison with research reports [15, 16]. The control of input parameters is done by a graphical user interface. The documentation is given in four volumes [17].

2.2 VTTBESIT (VTT)

The VTTBESIT code is a tool for numerical assessment of cracked and uncracked pipes, vessels, and weld joints. Both probabilistic and deterministic numerical simulations can be achieved by the VTTBESIT. In the probabilistic simulations leak, break, and risk can be computed. Specific cases (i.e. crack growth as a function of time due to fatigue) can be computed by deterministic approach.

Fracture mechanical simulations of cracks are done by the VTTBESIT on the basis of deterministic parameters i.e. crack size, orientation, and material properties. Elliptical or long crack shapes in both plate and cylindrical geometries can be simulated. Cracks orientation can be either axial or circumferential, and cracks can be located i.e. inside or outside of a cylinder. The degradation mechanisms, which are applicable so for by the VTTBESIT, are fatigue (low-cycle and high-cycle fatigue) and stress corrosion cracking. Each degradation mechanism can predict crack growth at different cycles or time for a given situation. Eventually, leak before break analysis can be performed by the VTTBESIT code, where leakage rate may be computed and compared to the detection threshold of a leak monitoring system.

Different sampling methods are used to perform probabilistic simulations such as Monte-Carlo, and Latin hypercube sampling (LHC). Load as a function of time, cycle, and location can be applied by a separate input file. The separate input file for loading enables one to apply any realistic loading in a more simplified manner.

For risk informed in-service inspections (RI-ISI), seven probabilities of detection (POD) curves are applicable by VTTBESIT, where out of the seven curves three by NUREG/CR-3869 [18] (advanced, good, poor) and four by WinPraise (advanced, very good, good, and marginal) [19].

The control of input parameters can be done by both graphical user interface and text files. Validations of the

VTTBESIT were done by reference cases from international benchmark activities, measurements of experimental investigations, and comparison with research report.

3 Definition of the example cases for comparative calculation

The design of the example cases for comparative analysis is based on previous benchmark activities. The inspection strategy and efficiency, however, are chosen consistently, rendering the single cases specific to this study. This approach for the simulation of in-service inspections is discussed in Sec. 3.3. An illustration of the cross sections of the different piping types is given in Fig. 2.

3.1 Fatigue Cases

Two different piping geometries are investigated, which are taken from the NURBIM benchmark study [1]. The original denominations, small pipe and medium pipe are kept. The fatigue growth of initial cracks is assumed. The simulations are understood to compute the leak probability of one specific welding position. For taking into account different influences on the presence of manufacturing defects at a given site, a specific defect density per weld is assumed. Thus, the results represent the absolute leak probability, rather than a conditional probability for a pre-cracked welding.

The two examples only differ by structural geometry, loading and initial cracks, while the material properties and crack growth assumptions are the same for both applications. Material properties are modeled as distributed parameters in many cases. The yield stress σ_y, ultimate tensile stress σ_t, and flow stress σ_f are assumed to be independently normally distributed, and the fracture toughness K_{IC} as well. Young's modulus E and the Poisson ratio ν are set to constant values. The parameters are listed in Table 3.

The cyclic crack growth rate (in mm/year) is described by a Paris law [20]

$$\frac{da}{dN} = C(\Delta K)^m \quad \text{or} \quad \frac{da}{dN} = C\frac{(\Delta K)^m}{\sqrt{1-R}}, \tag{1}$$

where ΔK is the stress intensity factor difference between maximum and minimum loads (in MPa $m^{1/2}$), and R is the ratio of minimal stress intensity factor to maximal, respectively. In the linear elastic regime, the stress intensity factor is proportional to the nominal stress, hence the R-ratio can be estimated well by the ratio of minimal and maximal stresses. While the choice of crack growth law is let open between the two formulas (the first is referred as Original Paris law, in contrast to the second, which is the Modified Paris law), the parameters $C = 5.06 \cdot 10^{-9}$ and $m = 3.93$ are fixed. The two curves are shown in Fig. 3.

The pipes outer diameter, D_0, thickness, t, and defect density per weld, Cρ, are shown in Table 1. The depth of initial crack is modeled by a log-normal distribution function, with location parameter, l, and scale parameter, s. The operation time of the pipes are assumed 40 years. The applied loads of the pipes are given in Table 2, where P_{bmin} is minimum primary stress, P_{bmin} is minimum secondary stress, P_{totmin} is minimum total stress, P_{bmax} is maximum primary stress, P_{emax} is maximum secondary stress, P_{totmax} is maximum total stress and Cy is load cycle per year. The time dependence of the cyclic stresses is visualized in Fig. 4 (sinusoidal shape assumed). In the graph, only the total stress (sum of primary and secondary parts) is given for simplicity. The minimal primary stress can be seen as a result of the dead weight, while the maximal primary stress is the sum of the dead weight and the membrane stress due to interior pressure. The secondary load can be interpreted as thermal expansion. In this context, the load history of the Small Pipe represent cycles

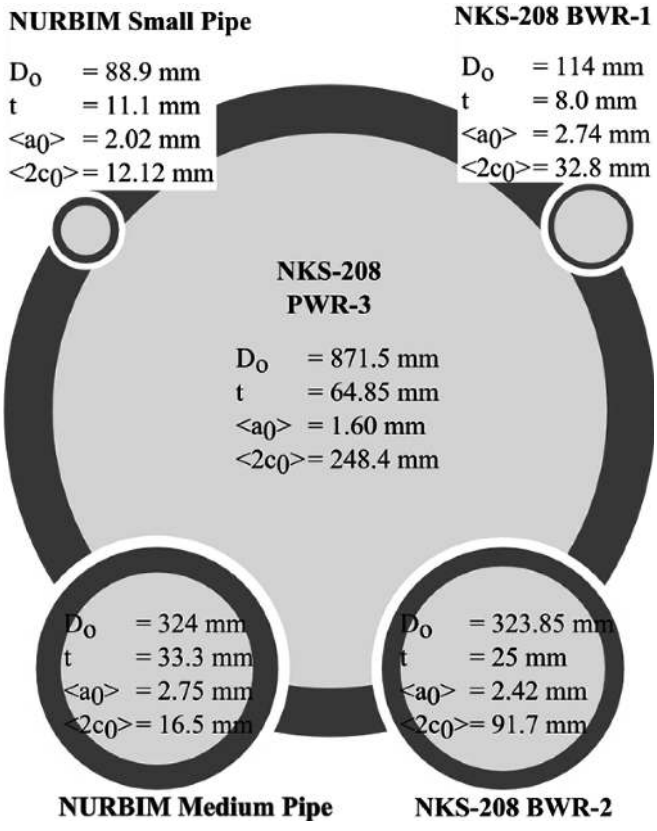

Fig. 2. Isometric comparison of the different example cases

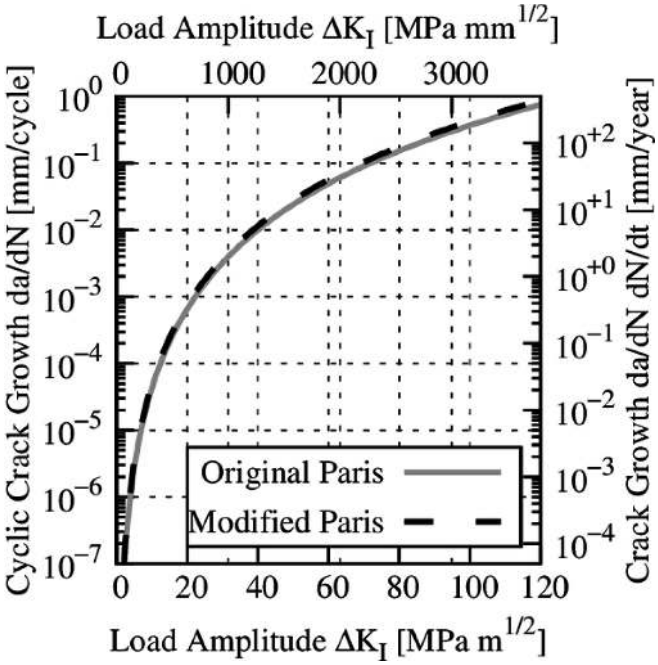

Fig. 3. Fatigue crack growth rates with Original and Modified Paris law. The latter, plotted for R = 0.25 and R = 0.3, are almost equal

of heat up and pressurizing, followed by cool-down and pressure release.

3.2 Corrosion Cases

The three different examples for corrosive crack initiation and crack corrosion cracking originate from [2]. They describe different components in BWR and PWR coolant lines. They differ in several details.

All assume an uncracked component at commissioning, and crack initiation is assumed to occur during operation. The timescale of the initiation in these examples is about 3700 years. In accordance to the previous study [2], an initiation rate per year of $2.687 \cdot 10^{-4}$ is chosen. Table 4 shows geometrical specifications of BWR-1, BWR-2 and PWR-3. As in the fatigue cases, the initial crack depth follows a log-normal distribution, while the initial crack length is exponentially distributed. The table contains the parameters of the depth-distribution and also μ_a and μ_l, the mean crack depth and length, respectively. The characteristic stresses (yield stress, σ_y, ultimate stress, σ_t) and the fracture toughness, K_{IC}, are modeled as normally distributed parameters. Young's modulus, E, the Poisson's ratio, ν, are deterministic. The prefactor, C, and the exponent, n, of the corrosion law are also constant. The parameters are shown in Table 5.

The operation time is set to 60 years, with 8000 operating hours per year. The stress corrosion cracking velocity (in mm/s) is governed by the equation

$$\frac{da}{dt} = C(\min\{K_I, K_{\text{sat}}\})^n \tag{2}$$

where K_I is the stress intensity factor (in MPa $m^{1/2}$), K_{sat} is a saturation value (set to 55.53 MPa $m^{1/2}$), and C and n are material dependent. The crack growth velocity is shown in Fig. 5.

The loading stresses in the cross section of the pipe depend on the radial coordinate r as well as on the azimuthal coordi-

Table 1. Pipe geometry and crack specifications for the NURBIM cases

	small pipe	medium pipe
D_0 [mm]	88.9	324
t [mm]	11.1	33.3
l [–]	0.5878	0.788
s [–]	0.485	0.67
$C\rho$	1.25×10^{-3}	0.01

Table 2. Loading conditions for NURBIM cases

	small pipe	medium pipe
P_{bmin} [MPa]	23.1	29.8
P_{emin} [MPa]	0.0	0.0
P_{totmin} [MPa]	23.1	29.8
P_{bmax} [MPa]	42.9	56.1
P_{emax} [MPa]	51.1	43.9
P_{totmax} [MPa]	94.0	100
Cy [–]	500	500
R -ratio [–]	0.25	0.3

Table 3. Material properties for the NURBIM cases, indicated values denote the mean value and the standard deviation of normal distributions

	NURBIM
E [GPa]	180
ν [-]	0.3
σ_y [MPa]	150 ± 15
σ_t [MPa]	450 ± 35
σ_f [MPa]	300 ± 16.8
K_{IC} [MPam$^{1/2}$]	265.7 ± 20

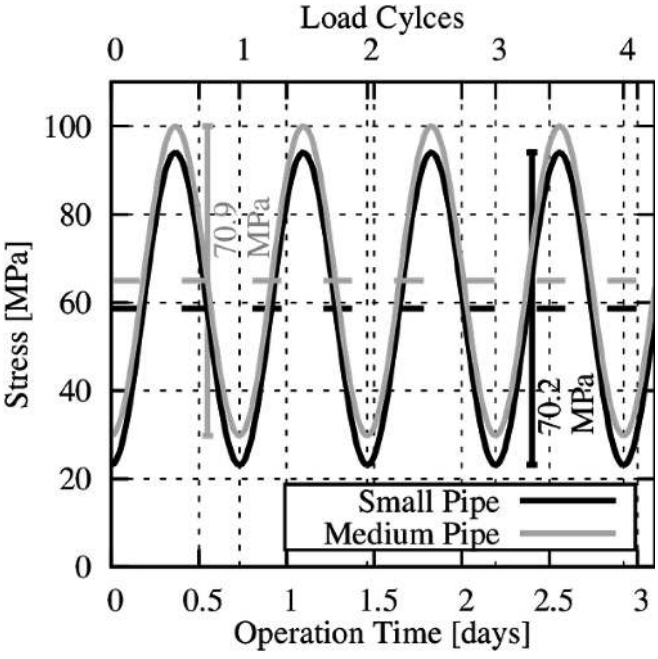

Fig. 4. Fatigue load cycles for the Small and Medium Pipe cases. Average load levels are shown as dashed lines

Table 4. Pipe geometry and crack specifications for the SCC cases

	BWR-1	BWR-2	PWR-3
D_0 [mm]	114	323.85	871.5
t [mm]	8	25	64.85
l [-]	0.9933	0.8179	0.3434
s [-]	0.1784	0.3672	0.4993
$C\rho$	2.687×10^{-4}	2.687×10^{-4}	2.687×10^{-4}
μ_a [mm]	2.743	2.424	1.597
μ_l [mm]	32.82	91.71	248.42

nate φ. The selected cases assume a combination of membrane stress σ_m, bending load σ_b, and residual stresses σ_{rs}, which can be written as

$$\sigma(r,\varphi) = \sigma_m + \sigma_b(r,\varphi) + \sigma_{rs}(r) \quad (3)$$

While the membrane stress is uniform and does not depend on the location, the bending part takes the form

$$\sigma_b(r,\varphi) = \sigma_B r\cos(\varphi). \quad (4)$$

In one case, an additional secondary bending term (prefactor P_e) is considered. The residual stresses are assumed to vary linearly through the wall. This simplification was already chosen in the previous analysis of these cases. It is described by the relation

$$\sigma_{rs}(r) = \sigma_{RS}\left(1 - 2\frac{r - r_i}{t}\right) \quad (5)$$

where r is the radial position measured from the pipe center, r_i is the inner pipe radius, and t is the wall thickness, respectively. The stress is tensile at the inner surface and compressive at the outer most position. The parameters of the assumed nominal stresses for BWR-1, BWR-2, and PWR-3 are given in Table 6, the stress variations are shown in Fig. 6.

Table 5. Material properties for the corrosion cases, the mean value and the standard deviation are shown for normal distribution functions

	BWR-1	BWR-2	PWR-3
E [GPa]	180	176	180
ν [–]	0.3	0.3	0.3
σ_y [MPa]	150 ± 15	125 ± 15	150 ± 15
σ_t [MPa]	450 ± 35	383 ± 30	450 ± 35
K_{IC} [MPa m$^{1/2}$]	265.7 ± 20	265.7 ± 20	265.7 ± 20
C [–]	1.46×10^{-12}	4.5×10^{-12}	1.46×10^{-12}
n [–]	3	3	3

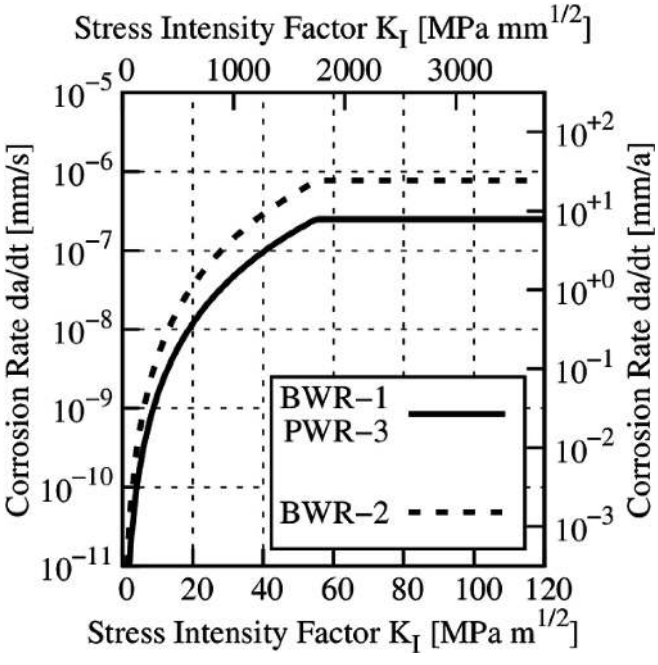

Fig. 5. Corrosive crack growth rates for the different example cases

3.3 In-Service Inspections and POD curves

The inspection during the operation is simulated in this study be assuming detection probabilities at given inspection time

Table 6. Loading conditions for SCC cases

	BWR-1	BWR-2	PWR-3
P [MPa]	7.0	7.0	15.41
σ_m [MPa]	20.0	19.2	40.4
σ_B [MPa]	11.0	18.6	51.1
P_e [MPa]	18.0	0.0	0
σ_{RS} [MPa]	233.0	50.0	100.0

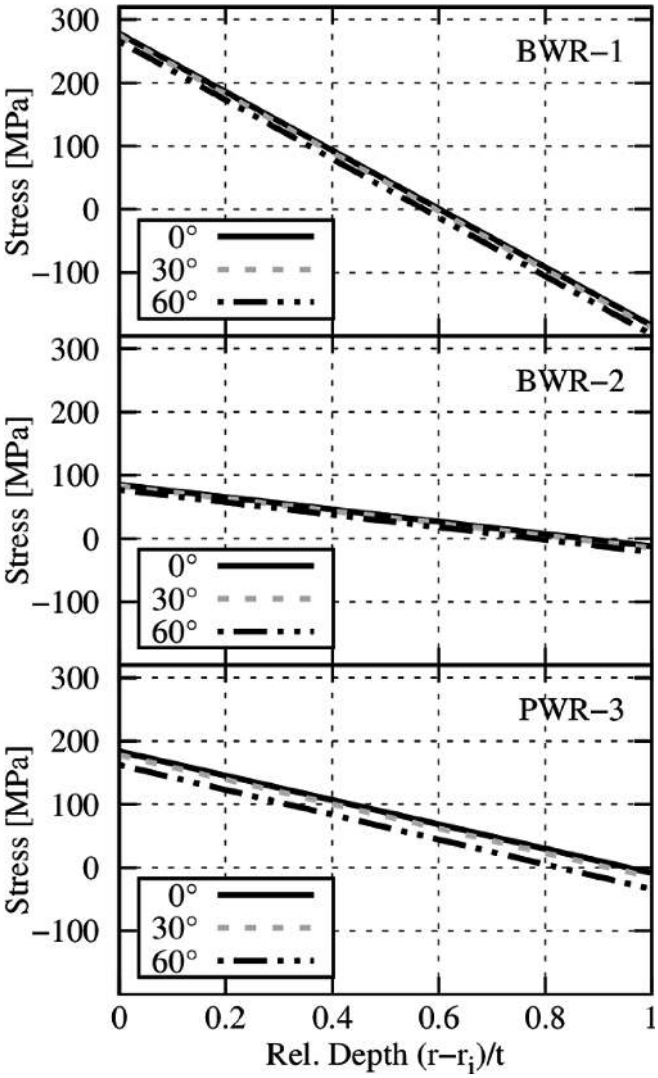

Fig. 6. Nominal stress distribution for the three corrosion cases BWR-1, BWR-2, and PWR-3. The denoted angle corresponds to the position relative to the point of maximal bending stress

intervals. The inspection interval is set to a 10-year period, with the first inspection after ten years in operation. This corresponds to a specific choice in [1]. In case of a detection, the component is assumed to be repaired, excluding any further failure in this case. This effect is modeled by probability of detection (POD) curves, which give the probability of detection as a function of the crack depth at inspection time.

In this study, the two families of POD curves are investigated, each containing different efficiencies. The NUREG familiy [18] takes the form

$$POD(a) = \Phi[\alpha + \beta ln(a/t)], \tag{6}$$

where α and β depend on the efficiency of the team. The WinPraise parametrization [19] of the POD curve differs, the equation reads

$$POD(a) = 1 - \varepsilon - \frac{1-\varepsilon}{2}\mathrm{erfc}\left[v \ln\frac{a}{ta*}\right]. \tag{7}$$

The inspection quality is modeled by appropriate choice of the parameters a^*, and v. The different parameter combinations for team qualities according to both parametrizations are shown in Table 7.

The different resulting POD curves are compared in Fig. 7. As it is expected, the probability of detection increases as the quality of a curve is higher. One main difference between the two parametrization families is the detectability of shallow cracks: While the presented WinPraise parametrizations (especially the low efficiency types) assume that the detection of cracks is unlikely if their depth is to small, the NUREG parametrizations start with higher detection probability for small relative crack depths. The poorest efficiency of all curves is modelled by the marginal WinPraise curve, while the NUREG-poor curve simulates a detection probability of 40 %-70 % for a wide range of crack depth. Curves of higher qualities (of both families) assume significantly higher detection probabilities for deep cracks. Realistic inspections performed by a well-trained team are modeled with the good and very good qualities, while the advanced parameters lead to POD curves which assume improvements of the present-day technologies.

Table 7. POD curve parameters for the NUREG (top) and WinPraise (bottom) family

NUREG		
quality	α	β
poor	0.432	0.163
good	3.75	0.583
advanced	3.63	1.106

WinPraise			
quality	a^*	ε	v
marginal	0.65	0.25	1.4
good	0.4	0.1	1.6
very good	0.15	0.02	1.6
advanced	0.05	0.005	1.6

4 Results

In this section, the results obtained by the authors using different codes are presented in common graphs, together with reference results from the previous studies. For a clear presentation, two graphs for each example case are presented, corresponding to the two POD curve families. In each of the plots, the quality is indicated by the line color, and the code which was used by the line type (dashed for PROST and dashed-dotted for VTTBESIT, respectively). Thus, for a comparison of the different codes, two curve with identical color and different dash type within one plot have to be compared. In this section, the pure observations of the single cases are documented. The analysis of the identified trends is found in Sec. 5.

4.1 NURBIM Small Pipe

The results for the Small Pipe case from the NURBIM fatigue benchmark are shown in Fig. 8 and Fig. 9, for NUREG and WinPraise detection curves, respectively. In addition to the annual leak frequencies, the computed failure probabilities at commissioning obtained by different participants of the benchmark [5] is shown, as well as the average leak probability during operation (the time dependency of annual leakage frequencies is not contained in the benchmark document).

If no inspection is performed, the failure probability is almost constant over the operation time, except for the very first year (elevated for PROST and reduced for VTTBESIT). The probability in the second/first year obtained by VTTBESIT and PROST is within the scattering of the NURBIM report for failure at commissioning. Up to year 10, all curves of one simulation code are on top of each other, since the first inspection which evaluates a POD curve takes place in this

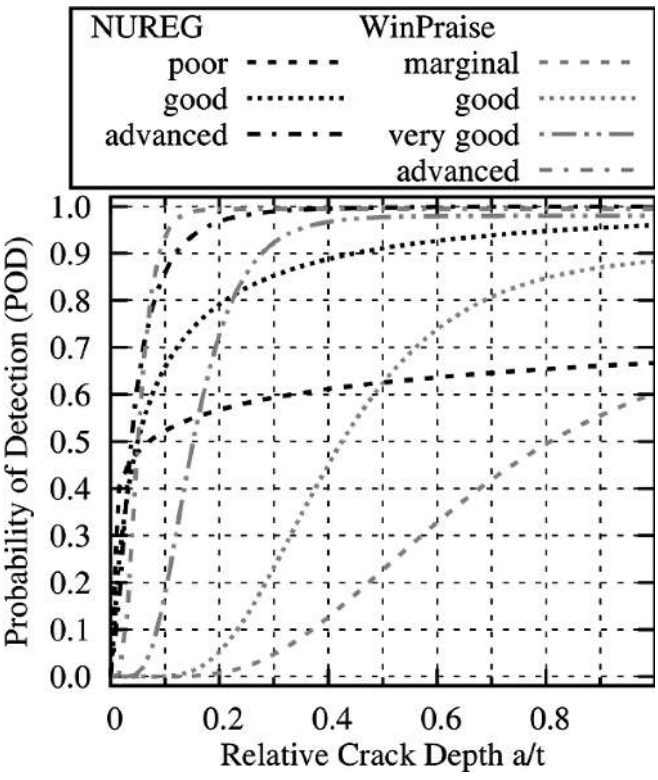

Fig. 7. Comparison of POD curves. Probability of detection as a function of the relative crack depth

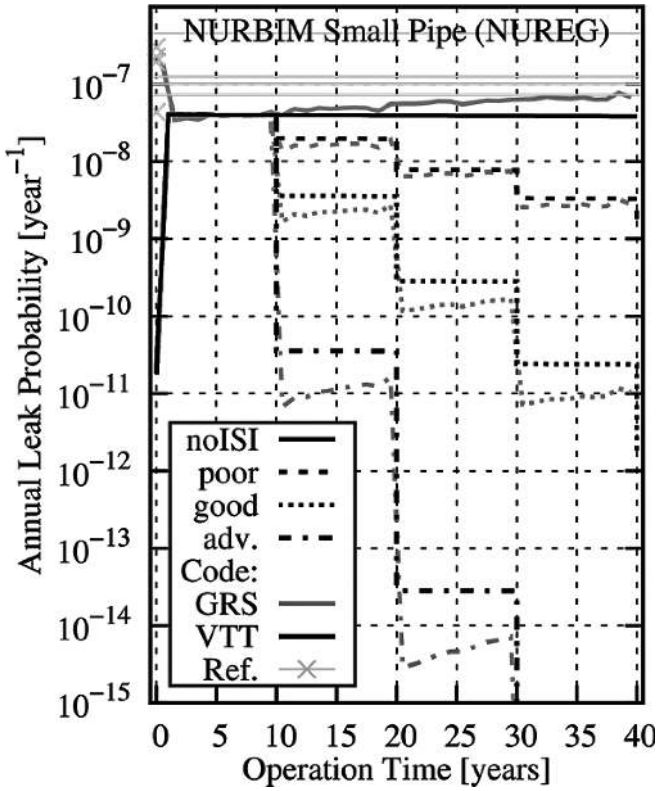

Fig. 8. Analysis of the yearly leak probability for the small pipe fatigue example. NUREG-POD curves for in-service inspections are applied

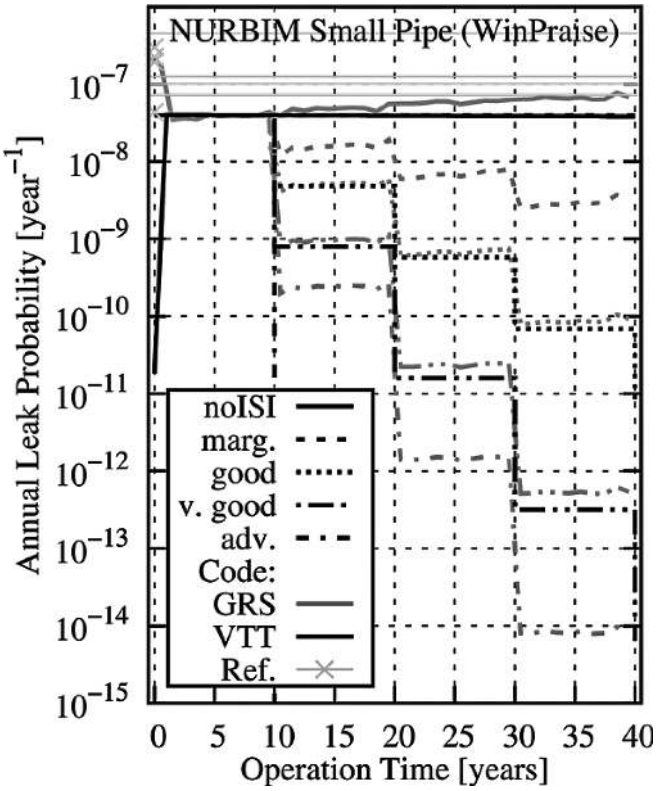

Fig. 9. Analysis of the yearly leak probability for the small pipe fatigue example. WinPraise-POD curves for in-service inspections are applied

year. This leads to the splitting of the resulting probability curves.

The effect of in-service inspections is clearly visible in the inspection years 10, 20, and 30, since the annual leaking probability drops according to the inspection efficiency. Beside one exception (VTTBESIT with WinPraise marginal POD curve), the presence of examinations lead to a decrease of the failure probability in the last ten years of more than one order of magnitude. The improved inspection models have a very pronounced effect, making leaks in the final years of the operation time very unlikely. The advanced method according to NUREG leads to smaller failure probabilities than the WinPraise curve. The poor/marginal method as well as the good methods from the NUREG and the WinPraise parametrization are very similar.

The agreement of PROST and VTTBESIT is good for the simulations without inspections, which find annual leak frequencies closer than the codes participating in the original benchmark study. The main difference is the increasing trend for PROST, and a (practically invisible) slight decrease for VTTBESIT. All three NUREG-POD curves lead to very coherent results for the two codes, same as the good and the very good WinPraise PODs. The marginal WinPraise POD leads to almost no decrease of the leak probability for VTTBESIT, while PROST observes a small effect. For WinPraise advanced results, a vanishing probability after the first application of the inspection for is calculated with VTTBESIT. These findings will be discussed in Sec. 5.6 in detail.

4.2 NURBIM Medium Pipe

The results for the Medium Pipe case of the NURBIM benchmark are shown in Fig. 10 and Fig. 11 for NUREG and WinPraise POD parametrizations, respectively. Again, the 0-year probability and the averaged leak probability per year from [1] is shown as comparison.

The behavior is similar to the Small Pipe case. The failure rate in the first year is the highest annual probability observed in the whole operation time, indicating that failures at commissioning are relevant. The failure probabilities at year 0 documented in the original report are in accordance with the finding. The rest of the operation time, is almost constant, the absolute values for the annual probabilities of both partners are close to each other, and are in the order of the mean annual probability found by the participants of the original benchmark. GRS finds that the failure probability in every year is between $1 \cdot 10^{-7}$ and $4 \cdot 10^{-7}$ without inspections, showing an increasing trend. VTT's leak probability does not rise with the time. This (almost) constant probability of leakage indicates that the number of fatigue cycles is small, and the stress range is low.

The inspection times lead to significant drops of the failure probability; each inspection acts like a shift of the curve by a factor, which depends on the efficiency of the inspection method. The least efficient method is the marginal curve of the WinPraise family. The advanced curve by NUREG is the most efficient one. Especially for the high-quality examinations, the total failure probability of the investigated component is dominated by events before the very first inspection, since further defects are very likely to be found already.

As for the simulations without inspections, VTT finds a steady continuation after each inspection step, while GRS finds an increasing leak probability after each inspection. The codes find similar results for the poor and the good NUREG parameters, and for the good and very good WinPraise parameters. VTT finds zero leak probability after one

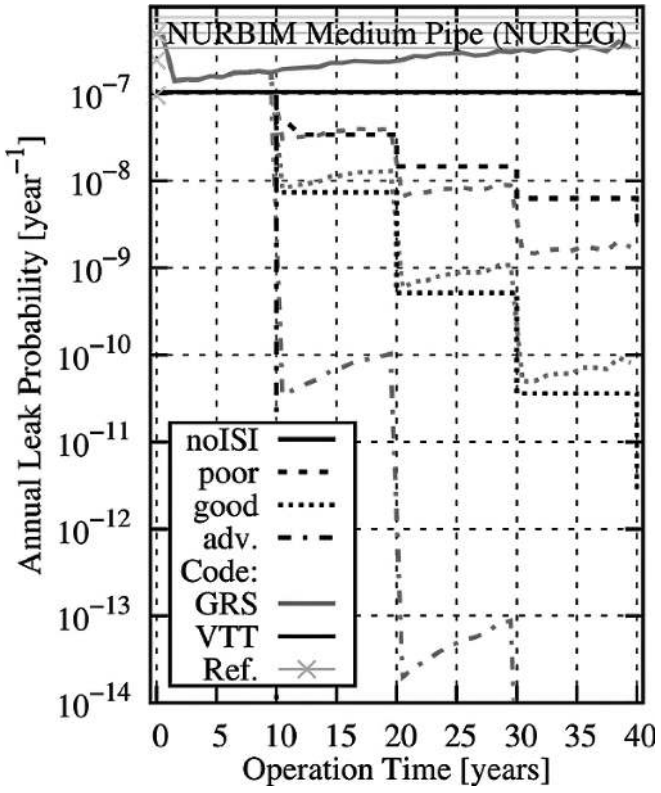

Fig. 10. Analysis of the yearly leak probability for the medium pipe fatigue example. NUREG-POD curves are investigated

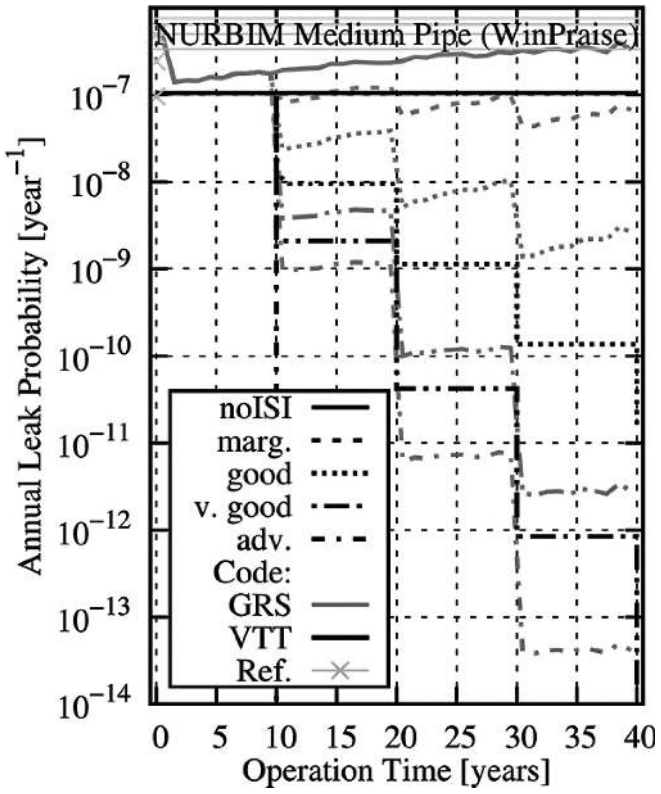

Fig. 11. Analysis of the yearly leak probability for the medium pipe fatigue example. The WinPraise method for in-service inspections is shown

inspection for both advanced parameters, and nearly no effect for the WinPraise marginal POD curve. The reasons for the differences are analyzed in Sec. 5, mainly in Sec. 5.6.

4.3 BWR-1

The analysis of the corrosion case BWR-1 is shown in Fig. 12 and Fig. 13, for both families of POD curves. The crack initiation frequency and the three reference results (without inspections) from the original report [2] are shown as well.

Since there are no initial cracks assumed, and crack initiation takes place during operation with the indicated frequency, the leak probability is very low in the first years. However, even after 10 years, when the first inspection takes place, the yearly failure rate is in the range of the initiation rate. This initiation frequency is the asymptotic value, which represent the equilibrium between crack initiation and failure of a pipe population. This time span of 10 years is very short, which is related to the thin wall of the BWR-1 example, i. e. the pipe is fastly penetrated by corrosive processes once a crack is initiated.

The failure probabilities (without in-service examinations) reported in the original report [2] differ significantly in the time when the steady state is reached: some 10 years, about 50 years, and even more is observed. In the first years, the PROST and VTTBESIT result without in-service inspections resemble two of the reference curves. For later times, the PROST curve without inspection (converges after about 10 years) resembles much one of the references. The VTTBESIT leak probability is decreasing for later times, with a maximal leak probability between 10–20 years. Such a behavior is also found for one refer-

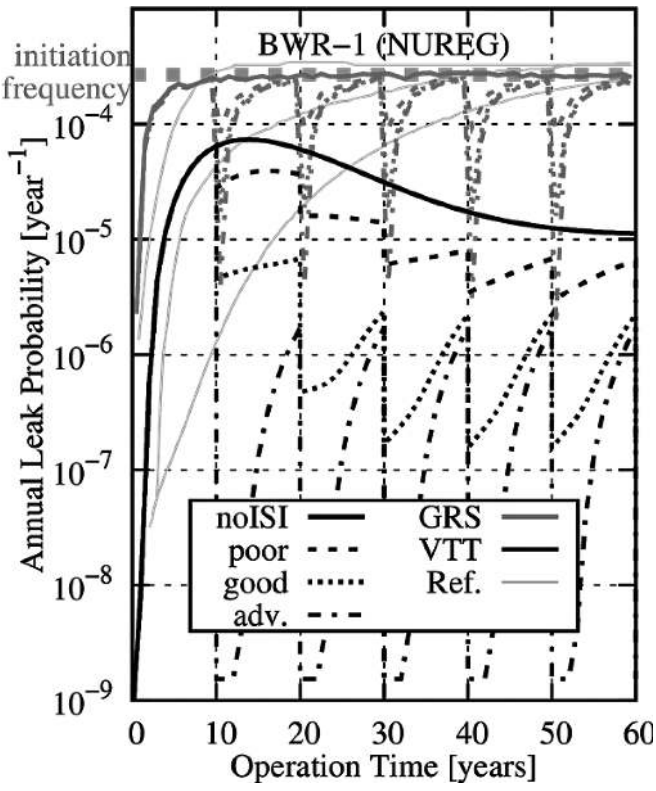

Fig. 12. Analysis of the yearly leak probability for the corrosion example BWR-1, the NUREG-POD curves are assumed for in-service inspections. Gray lines. PROST (GRS), black lines. VTTBESIT (VTT), thin gray lines. reference [2]. The dash type indicates the inspection quality

ence computation. The reasons for this behavior are discussed in Sec. 5.3 and Sec. 5.4.

The inspection times every 10 years are clearly visible in the plot, resulting in drops of the failure probability. However, the previous level of leak frequency is recovered quickly, due to the fast stress corrosion cracking mechanism. The different qualities of both POD families differ most in the year directly after the inspection.

For the NUREG POD curve family, the results of the VTT tool and the GRS tool are qualitatively similar. The poor POD parameters lead to a drop of the annual leak probability after an inspection by a factor of about 3–5. The increase of the yearly failing frequency is stronger for PROST than for VTTBESIT. With the good curve, both partners find a drop by a factor of about 10 after the first inspection, while later inspections have a stronger effect in the VTTBESIT result. For the advanced NUREG parameters, the most significant differences between the two codes appear.

The differences in the results using the WinPraise parametrizations of the POD curves are more pronounced. Marginal inspections have almost no effect in the VTT analysis, while GRS observes a decrease in leak probability by about a factor of two after each inspection. The good POD, instead, leads to a better leak prevention according to VTTBESIT than it is obtained with PROST. The quality levels very good and advanced lead to annual leak frequencies that differ even more. PROST finds that both qualities yield comparable results all over the time, while VTTBESIT reports a significant difference in the years directly after the inspection and a convergence thereafter. The analysis of the different inspection approaches of both codes is found in Sec. 5.6.

4.4 BWR-2

In Fig. 14 and Fig. 15, the BWR-2 example case is analyzed: Both inspection parametrization families are shown and compared to results (without inspections) in the benchmark documentation.

Unlike BWR-1, the increase of the leak probability per year is slower, which is directly related to the thicker pipe wall (see Fig. 2) and the lower level of residual stresses (see Sec. 3.2.2). Without inspections, the PROST as well as the VTTBESIT result are very similar, with slightly higher VTT leak probabilities in the first 10 years, and higher GRS probabilities in the last 50 years. After 15 years, the no-ISI curves of the two codes resemble one of the reference results from [2], while the others differ significantly more. The asymptotic value of the crack initiation frequency is not reached within the 60 years of operation.

In-service inspections lead to an enduring decrease of annual failure rates, the different qualities of POD curves lead to significantly different failure probabilities at future times. The least efficient POD function is the marginal WinPraise parametrization, the good method of NUREG and WinPraise are quite similar, while the lowest failure rates are obtained with the advanced NUREG parameters.

The NUREG POD parameter set results in similar curves of both partners. For all three qualities, the predicted probabilities of leakage in the year following an inspection of both partners are very close. The agreement of the two codes for one inspection quality is convincing especially for the first inspection (at 10 years), the differences become more pronounced for later inspections. It can be observed that the an-

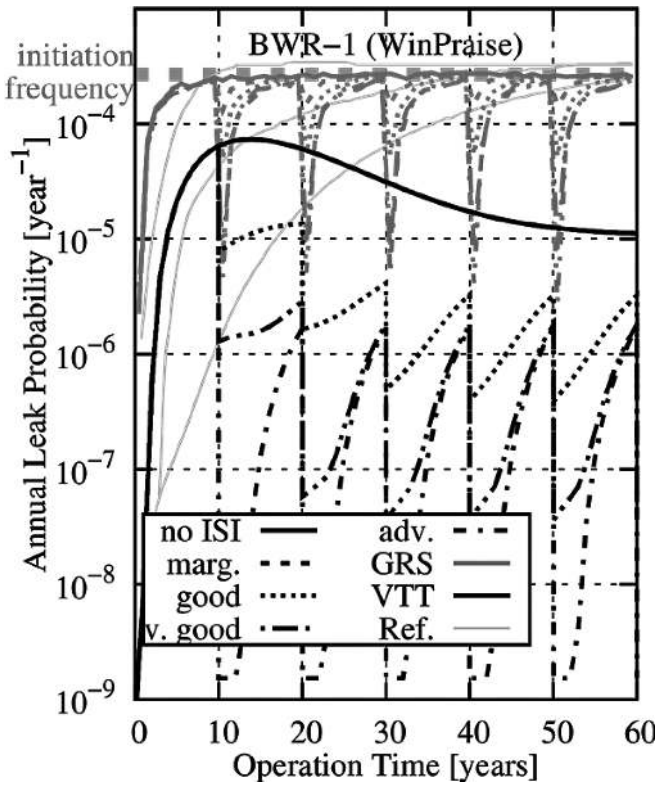

Fig. 13. Analysis of the yearly leak probability for the corrosion example BWR-1, the WinPraise POD curves are assumed for in-service inspections. Gray lines. PROST, black lines. VTTBESIT, thin gray lines. reference [2]. The dash type indicates the inspection quality

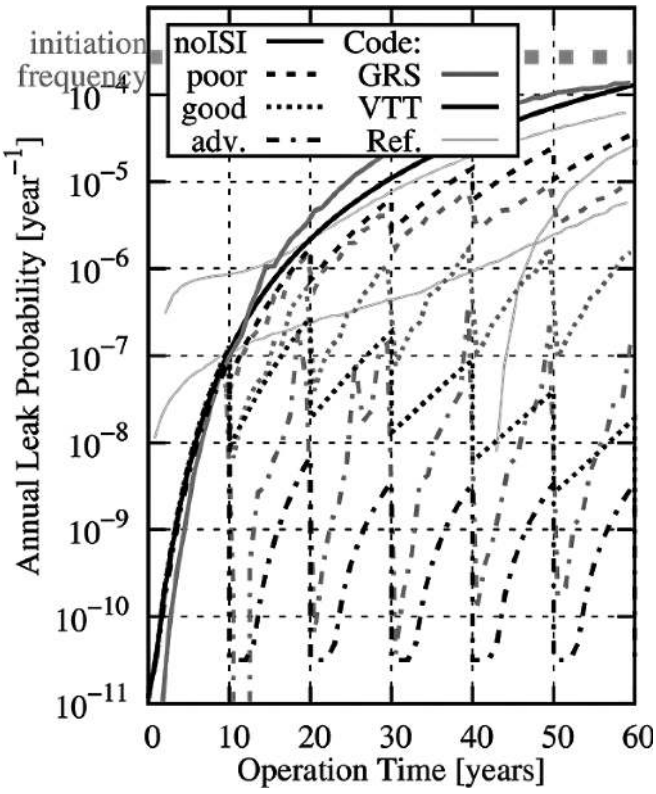

Fig. 14. Annual leak probability for the corrosion example BWR-2 (NUREG-POD curves); gray lines correspond to PROST/GRS, black lines to VTTBESIT/VTT, and thin gray lines to the reference results. The inspection (ISI) quality is indicated by the dash type

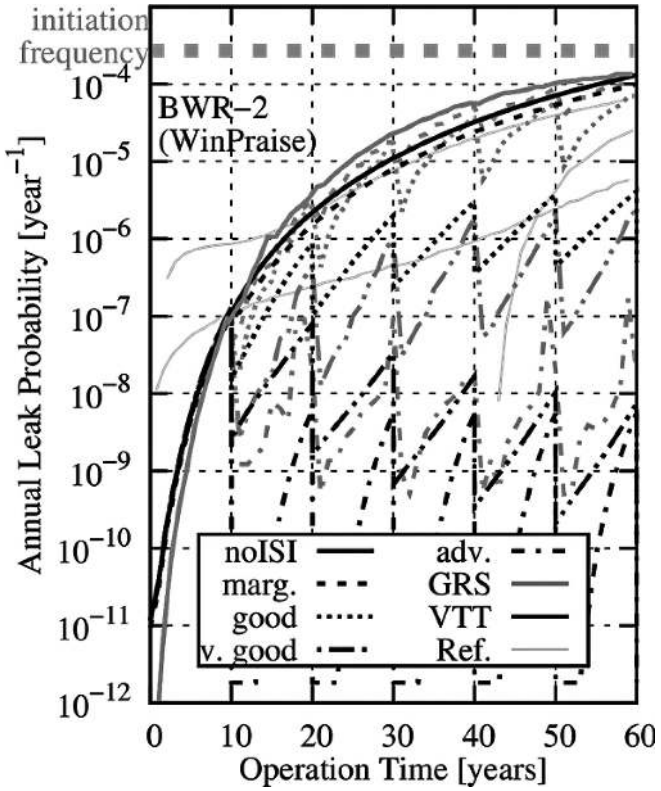

Fig. 15. Annual leak probability for the corrosion example BWR-2 (WinPraise curves); gray lines correspond to PROST, black lines to VTTBESIT, and thin gray lines to the reference results. The inspection (ISI) quality is indicated by the dash type

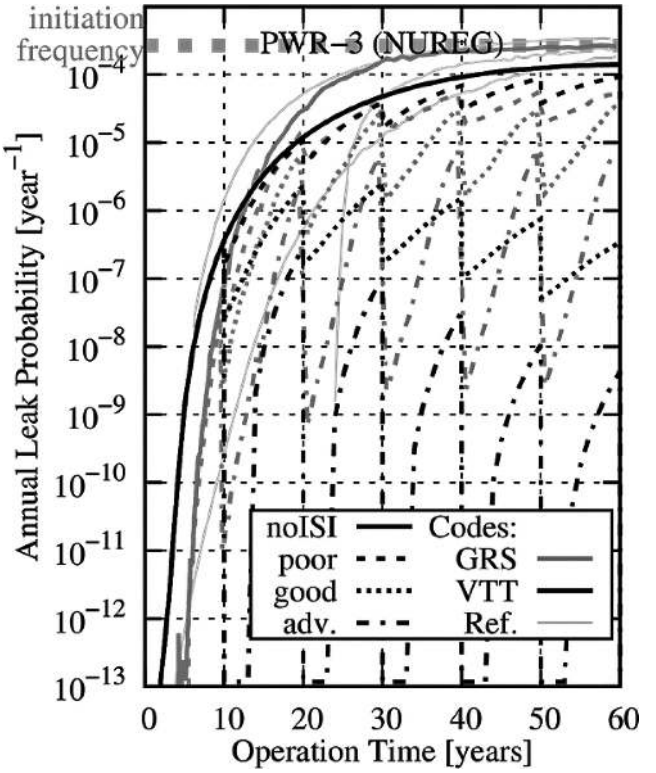

Fig. 16. Analysis of the annual leak probability for the corrosion example PWR-3, with different inspection quality levels assumed (NUREG-POD curves, coded by the line type). Black lines indicate VTTBESIT results (VTT), while gray lines belong to PROST (GRS), and thin gray lines to results from the original benchmark

nual leak frequencies grow faster between two inspections for the GRS result. VTT predicts a decreasing leakage probability trend for late years.

The findings for the WinPraise curves are slightly different. The marginal inspection quality has a minor, but visible effect in the VTTBESIT computation, while it is more explicit in the PROST simulation. The good and the very good quality level lead to leakage probability drops after each inspection which are larger for VTTBESIT than for PROST. This effect is the smallest at the first inspection, and become larger for later times. The advanced inspection POD curve results in clear differences between the two codes, but they remain roughly the same during the whole simulated operation time.

4.5 PWR-3

The case PWR-3 described in Sec. 3.2.4 is shown in Fig. 16 and Fig. 17. As a reference, the three probability curves without inspections from [2] are shown as well.

In this example, the leak probability per year without inspection is rising and attains values of the order of the asymptotic value (crack initiation frequency) within the operation time. The results of VTTBESIT and PROST without inspections are in good agreement, and are situated close to one of the reference curves. The other reference curves differ mainly in the first half of the simulated lifetime. In the first 15 years, VTTBESIT tends to predict higher leakage probability than PROST, while it is the other way round for later times. In-service inspections lead to oscillating failure rates; the level of the resulting probabilities depending on the inspection quality.

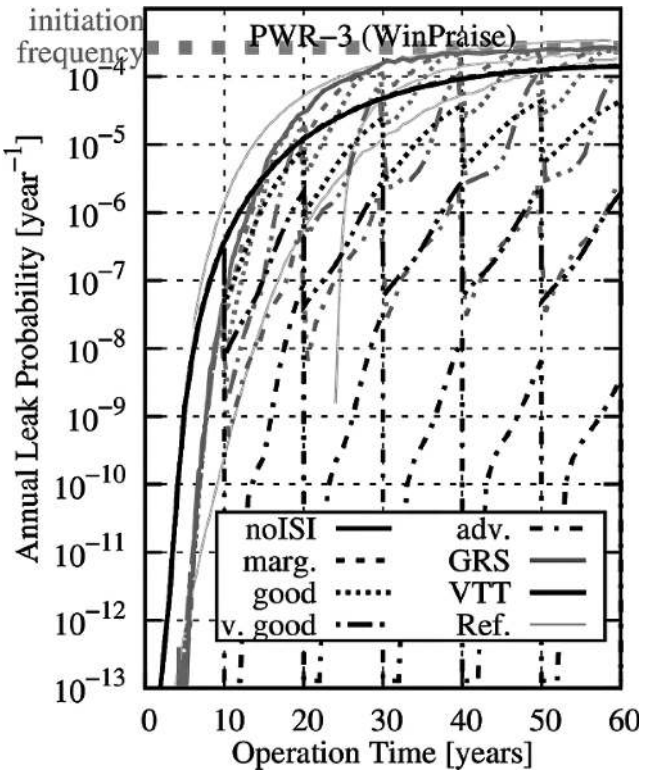

Fig. 17. Analysis of the annual leak probability for the corrosion example PWR-3, with different inspection quality levels assumed (WinPraise-POD curves, coded by the line type). Black lines indicate VTTBESIT results, while gray lines belong to PROST, and thin gray lines to results from the original benchmark

In the NUREG curve, the observations are similar to BWR-2. The two compared codes are in good agreement for the first inspection, the difference at this time might be explained by the small gap between the no-inspection results. For later times, the two approaches differ more and more, while the no-inspection curves converge.

In the PWR-3 case, the evolution of the yearly leak probability between two inspections differs visibly for NUREG curves and for WinPraise curves. In the last years before the next inspections, the leak probability grows much faster in the WinPraise curve. The differences between PROST and VTTBESIT for the WinPraise curves are similar to the previous cases. Again, the marginal quality leads to a small effect in the PROST result, and nearly to no effect in the VTTBESIT result. Higher qualities lead to a stronger deviations between the curves, however, there is no observed general trend for the after-inspection probability as in the BWR-2 case.

5 Discussion and comparative analysis

This section is dedicated to the discussion of the deviations between the results of the partners. After summarizing the observations, the different influences are discussed in the subsections.

5.1 Summary of observations

In the previous section, the results of all five cases were discussed. Concentrating on the comparison of the two tools VTTBESIT and PROST, some trends can be identified, which are common for all cases.

Both code's time evolution of the annual leak probability evidently differ in one point: The VTTBESIT curves are smooth (besides inspection intervals), while the PROST curves show partly a significant scattering. This volatile behavior is especially present at early times for the PROST code, while VTTBESIT has no difficulty to compute failure probabilities in the first operation years. Such behavior is intuitively related to the underlying probabilistic approach. This point is mainly discussed in Sec. 5.2.

Moreover, it is a common feature of all corrosion cases that PROST predicts higher leakage frequencies than VTTBESIT. Alternatively, this can be interpreted as earlier increase of the leakage probability according to PROST than it is deduced by VTTBESIT. This is an indication that the ageing mechanism in the GRS code acts faster than the VTT code throughout the stress corrosion cracking cases. An additional finding is the decrease of leak probabilities in the VTT code for later times, which is not predicted by the other code. The reasons for this findings are predominantly investigated in Secs. 5.3, 5.4, and 5.5.

Concerning the different inspection POD curves, there is another point. The NUREG parametrization leads to similar effects in both codes, while the results based on the WinPraise parametrization show important differences, especially for the low-quality level. The analysis of the treatment of in-service inspections is done in Sec. 5.6.

5.2 Probabilistics: Random variables and sampling

A key ingredient of the computation of the probability of leakage is the handling of statistically distributed variables. A number of approaches has been developed for the structural reliability context [16, 21, 22], which differ in stability, efficiency, and implementation effort. The temporal evolution of the annual leak probability as desired output poses a supplementary side condition, which excludes some approaches. Thus, the sampling strategy, relevant for selecting the values of random parameters for the simulation, might be responsible for systematic trends observed for one tool.

In the PROST computations, some parameters are prepared in advance in order to speed up the computations, and the conversion to correct parameters was performed analytically after the calculation. This concerns the crack existence frequency (for fatigue cases) and the initiation rate (for the corrosion cases): Only specimen are simulated which have cracks at some times during the simulation, uncracked pipes are omitted. The sampling is either done with simple Monte Carlo Sampling or with FORM-based importance sampling, thus importance sampling around the design point/most probable point. Usually about $5 \cdot 10^4$ simulations are performed for each curve.

The scattering of PROST's annual leak probability curves represents the fact that too few failure events were found by the algorithm in the corresponding years, and hence the remaining variance is visible. This effect is especially present in the early years of the corrosion cases, when the leak probability is small, because crack initiation and crack growth is required for leaks. In general, an increase of the total number of simulation would improve this behavior. In some cases, an additional simulation is run with a reduced operation time, and the result is used for the early times (first year up to 10–15 years).

In the VTTBESIT, the crack growth through the pipe wall is quantified with discrete degradation states. This approach allows the use of Markov process simulations to calculate leak and failure probabilities for piping components. The transition probabilities are assessed using the results from probabilistic fracture mechanic (PFM) simulations, which are performed with the VTTBESIT code. In the VTTBESIT simulations the sizes of the initial cracks are taken randomly from the respective probability density function, while all other input data variables are considered as deterministic. VTTBESIT results are used to construct a degradation matrix for the Markov process, in which crack growth leads into more degraded states, while inspections and subsequent repairs/replacements lead into less degraded states. For transition probabilities into less degraded states, POD functions are used. They are applied in the computations in the form of inspection matrices [23].

5.3 Material ageing: Stresses and K-factors

The degradation rapidity is influenced by the stress-intensity factors for both the fatigue cases and the corrosion cases. The stress intensity factors depend on the structural geometry, the loading conditions (stresses), and the defect configuration. Thus, the origin of deviations can be found in these three ingredients.

While the fatigue cases are modeled with uniform stress distributions in this study, the spatial dependence of crack-opening stresses is more involved for the corrosion cases (see Fig. 6). In these examples, high compressive forces at radia close to the outer radius are found: especially in the case BWR-1, and less pronounced for BWR-2 and PWR-3. These compressive stresses affect the crack tip of deep flaws, i.e. defects which have grown over some time. This behavior becomes more effective the more the crack grows through the wall, which reduces the leak probability as time passes. The decreasing leak probability for later times observed by one code can be explained by this relation: the strength of the

compressive forces (in combination with a thinner wall) is correlated with the decrease of the leak probability.

Both participating codes use analytical methods for the stress intensity factor computations. That means that the stress intensity factors are not calculated from a tailored FE analysis, but from an analytical formulation for the given geometry and loading condition. Such a formulation was usually done for specific geometries or within certain limits. In probabilistic simulations, distributed parameters may lead to extreme parameters, e. g. for crack sizes, which exceed the natural range of validity of analytical methods. It is important to identify these boundaries and the tendency of the simulations to cross them, in order to identify possible room for discrepancies.

For the circumferentially-oriented semi-elliptical cracks at the inner wall surface of a cylinder, both codes rely on the IWM formulation [12]. They are formulated as parametrized functions, with the stress given as 2-dimensional polynomial. It is computed for crack dimensions

$$c/a \in \{1, 4/3, 2, 5, 10\}, \quad a/t \in \{0.1, 0.2, 0.4, 0.6, 0.8\} \tag{8}$$

thus an interpolation between, and an extrapolation beyond the points is included in the approach. As pipe dimensions, $t/r_i \in \{0.1, 0.25\}$ are provided, all others have to be derived, e. g. by linear interpolation. The pipe dimensions and the mean crack aspect ratios of the different cases discussed in this study are listed in Table 8.

For the relative wall thickness t/r_i, only one case is close to the reference point, while three others are between, and one case is outside the interval. For the initial crack aspect ratio, two cases have mean values of depth and length which lead to ratios well above the reference points of the analytical approach. Hence, deviations of the stress intensity factors can be expected, even if the same compendium is used.

5.4 Crack growth: Velocity and numerical integration

The growth mechanisms for the assumed cracks in the five example cases are all formulated in terms of an ordinary differential equation for the crack size, see Eq. (1) and Eq. (2), respectively. While the initial conditions (at commissioning for the fatigue examples, at initiation for the corrosion examples) are fixed by the parameters, the integration of the crack growth over the operation time has to be done by the analysis tool. Efficient approaches ease the computation in the case that many simulation are necessary, which is the case for probabilistic studies.

The crack growth velocity itself results from the stress intensity factors, it is hence possible that different extrapolation prescription (see Sec. 5.3) lead to different results. The stopping condition of the integration, the time of leakage, is again subject for discussion in Sec. 5.5.

Table 8. The ratios of wall thickness and inner pipe radius t/r_i, and the ratios for the mean initial half crack length and mean initial crack depth c_0/a_0, for the studied examples

	t/r_i	c_0/a_0
small pipe	0.33	3
medium pipe	0.26	3
BWR-1	0.16	6
BWR-2	0.18	18.9
PWR-3	0.17	77.8

In the GRS code, the crack growth is summed by using a numerical solver with adaptive step size control. This means that neither fixed time steps (in case of corrosive crack growth) nor cylce-by-cycle summation (in case of fatigue growth) are used. Instead, the crack growth is calculated by the numerical integration of the ordinary differential equation (see Eq. (1) and Eq. (2), respectively) governing the time evolution of a flaw. The step size is controlled adaptively, steps are occasionally refined to preserve the desired precision, or to resolve the leakage time accurately. This approach is observed to be as efficient as stable.

As this works the best for constant load definitions during the operation, the three stress corrosion cracking cases were modified for the computation. The cases BWR-1, BWR-2, and PWR-3 assume 8 000 h of operation each year, thus there are operation interruptions. Although it is possible to model such changes in the loading in PROST, it was decided to downscale the crack growth velocity, in order to obtain a 8 000-hours-year. This improves the efficiency of the algorithm.

In the VTTBESIT, the time increment is fixed. The crack growth computation procedure by the VTT, takes into account the crack growth potential in all computation points along the crack front. During the simulation of a crack growth increment, the semi-elliptic area corresponding to the next crack size is computed first, by taking into account all crack growth vectors along the crack front. Then, the shape of the area is determined from the relation of the through wall and parallel to wall surface components of the crack growth vector [23].

5.5 Failure criteria: Thresholds and material properties

While a simulated crack is growing, the software has to check whether the surface crack will cause a leak at a given time or not. The information of the leakage time is the quantity that enters in the statistical evaluation presented in Sec. 4. Thus, the identified time has a direct influence of the failure evolution. If the criterion is more conservative, failures will happen earlier, and the curves will shift to the left, while best-estimate criteria will tend to predict later failures.

The simplest leak event criteria are solely based on the defect geometry: The critical depth is a parameter provided by the user. The natural choice $a/t = 1$ was chosen for consistency for both partners. However, this is not a very conservative decision, since the stress intensity factor formulation is not valid any more if $a/t > 0.8$. Failure criteria like $a > 80\% t$ or $a > 90\% t$ have been proposed and applied [2].

For taking into account (distributed) material properties, the critical depth or the failure of a defect can be estimated using more involved methods. For instance, the parameters of the cases are sufficient to apply the method of a failure assessment diagram (FAD) [11, 24]. The approach combines the assessment of the limit load with the fracture toughness.

The different possible leak criteria are compared in Fig. 18 for the three stress corrosion cracking cases. PROST simulations were performed with the 100 % and the 80 % criterion, as well as the FAD approach. Additionally, the material properties were assumed to be non-distributed in one case. The effect of the different criteria is rather small. The 80 % criterion leads to higher failures at earlier times, but it is a shift by few years. In case of BWR-1 (thin walls), it is practically invisible. The FAD application and the assumption of deterministic material properties have no effect in all three cases. This find-

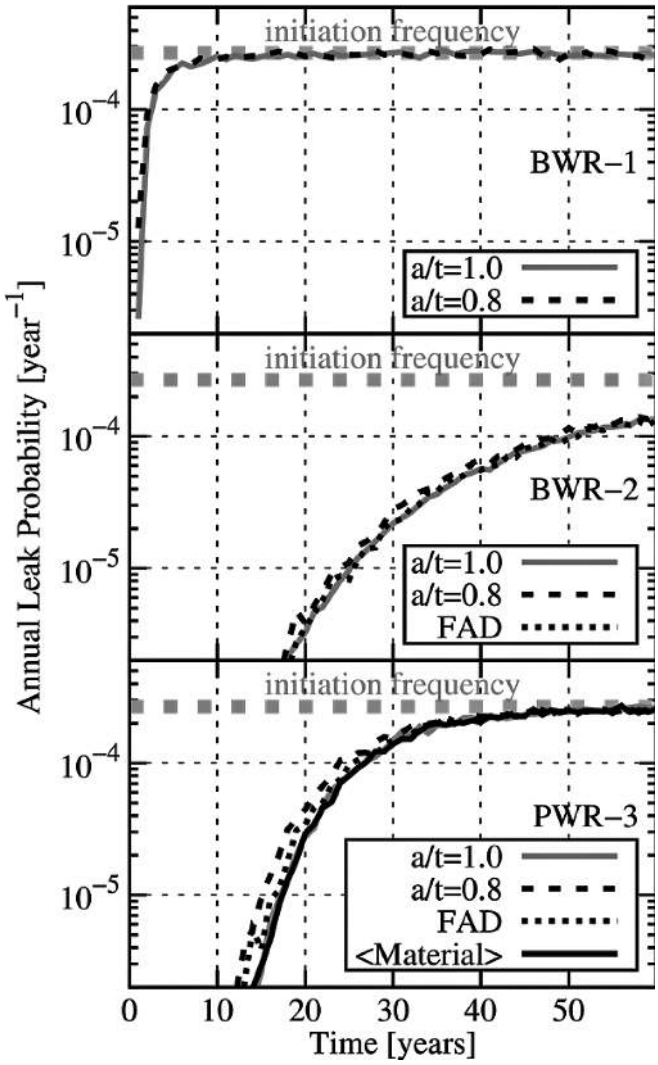

Fig. 18. Comparison of different leakage criteria for the cases BWR-1 (top), BWR-2 (center), and PWR-3 (bottom). No in-service inspections are simulated

ing justifies the deterministic treatment of material properties by VTTBESIT. The absence of influence by material properties and FAD approaches indicate that operational loadings of typical components of LWR are so low that cracks can become very deep before getting critical — so deep that the analytical methods assessing them are not strictly valid any more.

5.6 Inspections

In-service inspections are simulated in VTTBESIT and PROST by complementary approaches. While the first code uses a discrete-time Markov process on top of the fracture mechanical simulation, the latter tool decreases the individual parameter probability during the simulation. Thus, the characteristics of each POD curve (see Sec. 3.3) enter differently in both approaches.

Concerning the VTT approach, different discrete states in the Markov model correspond to different configurations of the inspected system. In this application concerning pipe degradation and inspections, these different states correspond to crack growth in in the pipe walls. Wall thickness is divided as a function of crack depth into states according to detection probabilities and assumed repaired policies. The overall method can be summarized as follow [25]: crack growth simulation based on PFM, construction of degradation matrix transition probabilities from PFM simulations and database analysis of crack initiation frequency, model for inspection quality, which used to construct inspection matrix transition probabilities, Markov model to calculate pipe rupture probabilities for chosen inspection schemes.

In contrast, PROST directly compares the relative depth of a crack at each inspection time with the POD curve, in each fracture mechanical simulation. The probability of detection for the current depth reduces the probability weight of the parameter set in case of a leak. Multiple inspections are assumed to be independent of each other.

With this background, deviations in the effects of in-service inspections can be expected. This conjecture is supported by the observation that the most important differences are found for the extreme POD curves: The advanced qualitiy of both families, and the marginal quality of the WinPraise parametrization.

6 Summary and outlook

In this comparative analysis, two fracture mechanical assessment tools developed and used by two different European TSOs were applied to a number of test cases. The designs examples covered BWR and PWR conditions, manufacturing defects and crack initiation, corrosive and fatigue crack growth, and in-service inspections. The results of former analyses were compared to the findings of this study.

The results of both partners are widely in good agreement with each other. Significant differences were mainly present for singular parameter combinations. The reasons for such systematic differences in the computed leak probabilities were identified in an extensive discussion. This analysis, based on the time-dependence of the annual leakage probability during operation, revealed the key ingredients relevant for the differing leak probability evolutions.

One of those aspects is the treatment of random variables and their probability, in the computation of the annual leak probabilities. The approaches of the two compared codes differ enough to explain differences in their results. Another source of deviations were in-service inspections in the two codes, which are considered in different ways by the two codes. Finally, the most apparent gaps between the results were found in examples with particular parameters (like extreme residual stresses, or unusually thin pipe walls), challenging the implemented analytical methods. In summary, these points are well understood.

The examination of the two software tools also identified factors which are in good coherence within the two partners, and quantities of minor influence. The fracture mechanics part of the tools, responsible for stresses, stress intensity factors, and crack growth, are modeled equivalently for both models. This is a satisfying finding, underlining the fact that the description of cracked components, usually a safety-relevant issue in nuclear industry, is done at an equally high level within the ETSON partners. This statement is the same for leak criteria; however, it could be quantified that different leak criteria only have a minor influence to the annual leak probability. This finding could be explained by the investigated loading scenario, which only considered operational loadings.

In the light of the ETSON research priorities [26], this study supports the development of computer tools for robust

numerical computations and reliable component design. The collaborative investigation of the safety analysis tools VTTBESIT and PROST can be seen as a part of the harmonization of European practices for structural lifetime and ageing assessment. The comparative study qualifies the applied softwares for the assessment of operating plants, as well as for new design purposes.

Acknowledgements

This work was partly performed in the framework of the German Reactor Safety Research and is funded by the German Federal Ministry of Economic Affairs and Energy (BMWi, project no. RS1516). This work was also partly prepared under the research project FOUND. The project is a part of SAFIR2015, which is a Finnish national nuclear energy program. FOUND work in 2015 was funded by the State Nuclear Waste Management Fund (VYR), Teollisuuden Voima Oyj (TVO) and Technical Research Centre of Finland (VTT).

(Received on 25 February 2016)

References

1 *Schulz, H.; Schimpfke, T.; Brickstad, B.; Chapman, V.; Sheperd, B.; Kelly, S.; Olsson, S.; Wintle, J.; Muhammed, A.; Simola, K.*: Nuclear Risk-Based Inspection Methodology for passive components (NURBIM). Final Report, Contract FIKS-CT-2001-00172, August 2004
2 *Simola, K.; Cronvall, O.; Männistö, I.; Gunnars, J.; Alverlind, L.; Dillström, P.; Gandossi. L.*: Studies on the effect of flaw detection probability assumptions on risk reduction at inspection. Nordic nuclear safety research, NKS-208, December 2009
3 *Simonen, F. A.; Doctor, S. R.; Gosselin, S. R.; Rudland, D. L.; Xu, H.; Wilkoski, G. M.; Ladell, B. O. Y.*: Probabilistic Fracture Mechanics Evaluation of Selected Passive Components. Technical Letter Report PNNL-16625, Pacific Northwest National Laboratory, May 2007
4 *Marie, S.; Faidy, C.*: BENCH-KJ – Benchmark on the analytical evaluation of the fracture mechanic parameters K and J for different components and loads. OECD IAGE, Rev. 5, March 2013
5 *Marie, S.*: BENCHKJ : Benchmark on analytical methods for the Fracture Mechanics parameters calculation. 2012 progress report SEMT/LISN/RT/12–038/A, CEA, December 2012
6 *Marie, S.; Faidy, C.*: Bench-KJ: Benchmark on analytical calculation of fracture mechanics parameters K and J for cracked piping components – progress of the work. Proceedings of the ASME 2013 PVP Conference, July 2013, DOI:10.1115/pvp2013-97178
7 *Kayser, Y.; Marie, S.; Chapuliot, S.; Le Delliou, P.; Faidy, C.*: Bench-KJ: Benchmark on analytical calculation of fracture mechanics parameters K and J for cracked piping components – final results and conclusions. Transactions, SMiRT-23, August 2015
8 Components of the Reactor Coolant Pressure Boundary of Light Water Reactors. Safety Standards of the Nuclear Safety Standards Commission, Parts 1–4, November 2012
9 Verification Analysis for Rupture Preclusion for Pressure Retaining Components in Nuclear Power Plants. Safety Standards of the Nuclear Safety Standards Commission, November 2014
10 ASME Boiler & Pressure Vessel Code. Vol. XI: Rules for In-service Inspection of Nuclear Power Plant Components. The American Society of Mechanical Engineers, 2013
11 Assessment of the Integrity of Structures Containing Defects. R6-Revision 4, April 2001
12 *Busch, M.; Petersilge, M.; Varfolomeyev, I.*: Polynomial Influence Functions for Surface Cracks in Pressure Vessel Components. IWM-Report Z 11/95, October 1995
13 *Zahoor, Z.*: Ductile fracture handbook. Vol. 1–3, EPRI-Report NP-6301-D, 1989–1991
14 *Heckmann, K.; Bläsius, C.; Bahr, L.; Sievers, J.*: WinLeck 4.7. User's Manual and Validation Report. GRS-P-6 Vol. 1–2 Rev. 5, June 2015
15 *Heckmann, K.; Sievers, J.*: Code development for piping integrity assessment with respect to new German safety standard. Transactions SMiRT-23, Div. II, Manchester, August 2015
16 *Heckmann, K.; Ma, K.; Sievers, J.*: Probabilistic aspects on break preclusion assessment in nuclear piping. Proceedings of the 41th MPA-Seminar, Stuttgart, October 2015
17 *Heckmann, K.; Bläsius, C.; Ma, K.; Sievers, J.*: PROST 4.4. User's Manual, Theory Manual, Validation Report, Programmer's Manual. GRS-P-7 Vol. 1–4, Rev. 5, June 2015
18 *Simonen, F. A.; Woo, H. H.*: Analyses of the Impact of Iservice Inspection Using a Piping Reliability Model. NUREG/CR-3869, PNL-5149, July 1984
19 *Harris, D. O.; Dedhia, D. D.*: WinPRAISE 98 PRAISE Code in Windows. Engineering Mechanics Technology, Inc., 1998
20 *Paris, P. C.; Erdogan, F.*: A Critical Analysis of Crack Propagation Laws. Journal of Basic Engineering; Transaction, American Society of Mechanical Engineers, Series D, 85, PP. 528–534, 1963
21 *Abdo, T.; Rackwitz, R.*: Reliability of uncertain systems. Finite Elements in Engineering Applications, 161–176, INTES, Stuttgart 1990
22 *Vepsä, A.; Cronvall, O.*: Comparison of three sampling methods in the context of probabilistic fracture mechanics analyses of NPP piping welds: case study. Research report VTT-R-00152–10, VTT, 2010
23 *Cronvall, O.; Alhainen, J.; Kaunisto, K.; Männistö, I.; Silvonen, T.; Vepsä, A.*: RI-ISI Analyses and Inspection Reliability of Piping Systems (RAIPSYS). RAIPSYS project Summary Report, Technical Research Centre of Finland (VTT), Espoo, Finland, 2013.
24 *Kocak, M.*: European Fitness For Service Network. FITNET Final Technical Report, GKSS Forschungszentrum, GTC1-2001-43049, 2006
25 *Cronvall, O.; Männistö, I.; Simola, K.*: Development and testing of VTT approach to risk-informed in-service inspection methodology. Final report of SAFIR INTELI INPUT Project RI-ISI, Technical Research Centre of Finland (VTT), Espoo, Finland, 2007
26 Position Paper of the Technical Safety Organisations: Research Needs in Nuclear Safety for Gen2 and Gen3 NPPs. ETSON/2011-001, October 2011

The authors of this contribution

Dr. rer. nat. *Klaus Heckmann* (corresponding author)
E-Mail: Klaus.Heckmann@grs.de
Gesellschaft für Anlagen- und Reaktorsicherheit gGmbH
Schwertnergasse 1
D-50667 Cologne
Germany

M.Sc. *Qais Saifi*
VTT Technical Research Centre of Finland
Kemistintie 3 Espoo, P.O. Box 1000
FI-02044
Finland

Bibliography
DOI 10.3139/124.110725
KERNTECHNIK
81 (2016) 5; page 484–497

ISSN 0932-3902